Published in final edited form as:
Biochem Pharmacol. 2012 May 15; 83(10): 1456–1464. doi:10.1016/j.bcp.2012.02.010.

Antitumor activity of a novel STAT3 inhibitor and redox modulator in non-small cell lung cancer cells☆

Xiaoying Liu[a], **Wei Guo**[a], **Shuhong Wu**[a], **Li Wang**[a], **Ji Wang**[a], **Bingbing Dai**[a], **Edward S. Kim**[b], **John V Heymach**[b], **Michael Wang**[c], **Luc Girard**[d], **John Minna**[d], **Jack A. Roth**[a], **Stephen G. Swisher**[a], and **Bingliang Fang**[a,*]

[a]Department of Thoracic and Cardiovascular Surgery, the University of Texas MD Anderson Cancer Center, Houston, TX, 77030, USA

[b]Department of Thoracic and Head and Neck Medical Oncology, the University of Texas MD Anderson Cancer Center, Houston, TX, 77030, USA

[c]Department of Lymphoma and Myeloma, the University of Texas MD Anderson Cancer Center, Houston, TX, 77030, USA

[d]Hamon Center for Therapeutic Oncology, The Harold C. Simmons Comprehensive Cancer Center, University of Texas Southwestern Medical Center, Dallas, TX, 75390, USA

Abstract

NSC-743380 is a novel STAT3 inhibitor that suppresses the growth of several NCI-60 cancer cell lines derived from different tissues and induces regression of xenograft tumors *in vivo* at various doses. To evaluate the antitumor activity of NSC-743380 in lung cancer cells, we analyzed the susceptibility of 50 NSCLC cell lines to this compound using cell viability assay. About 32% (16 of 50) of these cell lines were highly susceptible to this compound, with a 50% inhibitory concentration (IC_{50}) of <1 μM. In mechanistic studies, the increased numbers of apoptotic cells as well as increased PARP cleavage showed that cytotoxic effects correlate with apoptosis induction. Treatment with NSC-743380 inhibited transcription factor STAT3 activation and induced ROS production in sensitive human lung cancer cell lines but not in resistant cells. Blocking ROS generation with the antioxidant NDGA dramatically abolished NSC-743380-induced growth suppression and apoptosis, but had minimal effect on NSC-743380-induced STAT3 inhibition, suggesting that STAT3 inhibition is not caused by ROS production. Interestingly, knockdown of STAT3 with use of shSTAT3 induced ROS generation and suppressed tumor cell growth. Moreover, scavenging ROS induced by STAT3 inhibition also diminished antitumor activity of STAT3 inhibition. *In vivo* administration of NSC-743380 suppressed tumor growth and p-STAT3 in lung tumors. Our results indicate that NSC-743380 is a potent anticancer agent for lung cancer and that its apoptotic effects in lung cancer cells are mediated by induction of ROS through STAT3 inhibition.

Keywords

Drug development; Lung Cancer; STAT3; Reactive oxygen species

☆*Grant support:* This work was supported in part by the National Institutes of Health through R01 CA092481 and R01 CA124951 to B. Fang, Specialized Program of Research Excellence (SPORE) grant CA070907, The University of Texas MD Anderson Cancer Center Support grant CA-016672, Lung Program, Nuclear Magnetic Resonance, DNA Analysis and Flow Cytometry, and Cellular Imaging Core Facility, and William Burchenal Memorial Research Fund.

*Corresponding author. Tel.: +1 713 563 9147; fax: +1 713 794 4901. bfang@mdanderson.org (B. Fang).

1. Introduction

Signal transducer and activator of transcription 3 (STAT3) is a member of a family of latent cytosolic transcription factors whose activation is contingent on the phosphorylation of the conserved tyrosine residue (Y705) by upstream kinases [1]. Constitutive activation of STAT3 has been detected at high frequency in diverse human cancer cell lines and tumors, such as lung, prostate, ovarian, pancreatic, skin, and breast cancers [2]. STAT3 activation leads to increased expression of downstream targets and increased cell survival, proliferation, and tumor growth *in vivo* [3]. Inhibition of STAT3 results in increased apoptosis, decreased proliferation, and decreased tumor size [3–5]. Thus, targeting the STAT3 signaling pathway could provide an important approach in anticancer therapy.

Reactive oxygen species (ROS) and cellular oxidative stress have been associated with cancer for a long time. However, the nature of this association is both complex and paradoxical. For example, oxidants are required for tumor cell growth, and yet oxidative stress can possibly be exploited therapeutically [6]. This can be further explained as follows: under normal physiologic conditions, healthy cells maintain redox homeostasis. An increase of ROS may promote cell proliferation and survival, as in the case of many cancer cells, which are documented that ROS is responsible for initiation, progression, invasion and metastasis of cancers [7,8]. However, when ROS increases to a high level, it may overwhelm the antioxidant capacity of the cell and trigger the cell death process [9]. Therefore, inducing the generation of ROS or inhibiting the cellular antioxidant system to trigger cancer cell death is a strategy shared by all nonsurgical therapeutic approaches for cancers, including chemotherapy, radiotherapy, and photodynamic therapy [10,11].

Recently, we identified a small molecule, oncrasin-1, that effectively kills various human lung cancer cells with the KRAS mutation by disrupting the RNA processing machinery [12,13]. We also developed and evaluated a series of novel derivatives based on the structure of oncrasin-1 [14]. In our initial testing, two of our compounds, in particular, NSC-741909 and NSC-743380, were especially potent in their anticancer activity. Our previous study showed that NSC-741909 can induce ROS generation and subsequent JNK activation, which was one of the mechanisms of NSC-741909-mediated antitumor activity [15,16]. Although NSC-741909 and NSC-743380 have similar anticancer efficacy *in vitro* [14], NSC-743380 has much better anticancer efficacy *in vivo* and a better safety profile than NSC-741909 has, which makes NSC-743380 more suitable for further evaluation as an anticancer agent. Our recent study showed that NSC-743380 suppressed STAT3 activation in breast and renal cancer cells, which is associated with the susceptibility of renal and breast cancer cells to this compound.

In the current study, we further investigated the anticancer activity and mechanisms of NSC-743380 in lung cancer cells. Our results showed that NSC-743380 is highly active against a number of cancer cell lines derived from NSCLC lung cancer. Mechanistic studies demonstrated that NSC-743380 induced a dramatic increase in ROS and down-regulated p-STAT3 in its sensitive cell lines. We also found that suppression of STAT3 is sufficient to induce ROS generation and cytotoxicity in lung cancer cells. Our results suggested that STAT3 inhibition is one of the major mechanisms of action by NSC-743380.

2. Materials and methods

2.1. Cell lines and cell culture conditions

The 50 human NSCLC cell lines, including H460, H157, H1299, and H322, were propagated in a monolayer culture in Dulbecco's Modified Eagle's Medium supplemented with 10% fetal bovine serum, 100 units/mL penicillin, and 100 μg/mL streptomycin. Normal

human bronchial epithelial (HBEC3KT) [17] cells were grown in keratinocyte serum-free medium (Invitrogen, Grand Island, NY) with supplements for keratinocyte-SFM and antibiotics. The medium and antibiotics were from Invitrogen. All cells were maintained in a 37 °C incubator with 95% humidity and 5% CO_2.

2.2. Chemicals and antibodies

NSC-743380 was synthesized in our laboratory as described previously [14]. This compound was 98.5% pure, as determined by high-performance liquid chromatography-mass spectrometry analysis. The chemical structure was confirmed by nuclear magnetic resonance assay. The NDGA was purchased from Calbiochem (Rockland, MA) and the 2′, 7′-dichlorofluorescein diacetate (H_2DCF-DA) from Invitrogen Molecular Probes. Antibodies for Western blot analysis were obtained from Cell Signaling Technology (Beverly, MA), except for β-actin, which was acquired from Sigma (St Louis, MO). Secondary antibodies were purchased from Li-Cor Corp (Lincoln, NE).

2.3. ROS analysis

The cell-permeable nonfluorescent compound H_2DCF-DA was used for measuring intracellular ROS generation, as previously described [15]. Briefly, the day before the assay was performed, cells were seeded at a density of 3×10^5 per well of six-well plates. The cells were treated either with various concentrations of NSC-743380 for 6 h or with 1 μM NSC-743380 for different time points, *i.e.,* 0.5, 2, and 6 h, respectively. In the NSC-743380-antioxidant combination experiments, the antioxidant was added 1 h before NSC-743380 was added. H_2DCF-DA was dissolved in DMSO and diluted with pre-warmed phosphate-buffered saline (PBS) to a final concentration of 5 μM. After treatment with NSC-743380, the growth media was replaced with PBS containing the probe. After incubation for 40 min at 37 °C, cells were returned to a pre-warmed growth medium and incubated at 37 °C for 10 min. Cells were trypsinized and washed with pre-warmed PBS once. The samples were then subjected to a flow cytometry assay using a FACS Caliber (BD Biosciences, San Jose, CA). The flow cytometry assays were performed at the Flow Cytometry and Cellular Imaging Facility at The University of Texas MD Anderson Cancer Center. All experiments were performed at least twice.

2.4. Apoptosis analysis

Apoptotic cells were analyzed by flow cytometry with use of propidium iodide staining (BD Biosciences). In brief, cells were seeded at a density of 3×10^5 per 6-cm dishes, allowed to grow overnight, and then treated with 0.3 μM or 1 μM NSC-743380 alone or in combination with antioxidants for 24 h. The antioxidants were added to the cells 1 h before NSC-743380 was added. After the treatment, cells were harvested with trypsin, washed once with PBS, and then fixed with 70% ethanol overnight at 4 °C. Cell pellets were harvested and resuspended with 500 μL of 50 μg/mL propidium iodide containing RNase. Cells were stained at room temperature for 30 min in the dark. Sub-G0/G1 cellular DNA content was then measured with use of flow cytometry and Cell Quest software (BD Biosciences). All experiments were performed at least twice.

2.5. Cell viability assay

Cells were seeded at a density of 4000 cells/well in 96-well plates. After overnight incubation, the cells were treated for 72 h with NSC-743380 (0–31 μM), either alone or in combination with antioxidants that were added to the cells 30 min before NSC-743380 was added. The inhibitory effects of NSC-743380 alone or with antioxidants were determined by using the sulforhodamine B assay (SRB assay), as described previously [18].

2.6. shRNA and transient transfections

shRNA constructs in pLKO.1 vector specifically targeting human STAT3 sequences were purchased from Open Biosystems (Lafayette, CO). Control cells were transfected with pLKO.1 vector. Cells were transfected with shRNA by using Lipofectamine 2000 (Invitrogen) per the manufacturer's instruction. At 48 h after transfection, cells were harvested either for ROS generation analysis or for Western blot analysis.

2.7. Western blot analysis

Western blot analysis was performed to analyze protein expression and phosphorylation after cells were treated with NSC-743380 alone or combined with antioxidants, or after specific knockdown of STAT3. Briefly, cells were washed in PBS, collected, and then lysed in RIPA buffer (radioimmunoprecipitation assay buffer, Tris–Cl 50 mM; NaCl 150 mM; SDS 0.1%; Na-deoxycholate 0.5%; NP40 1%) containing proteinase inhibitor cocktail and phosphatase inhibitor cocktail (Roche Applied Science, Indianapolis, IN). The lysate was centrifuged at 10,000 × *g* at 4 °C for 10 min. The supernatant (50–100 μg of protein) was fractioned by SDS-PAGE using 10% gels and was electrophoretically transferred to Hybond-enhanced chemiluminescence membranes (GE Healthcare Life Sciences, Piscataway, NJ). The membrane was blocked with blocking buffer (Li-Cor) at room temperature for 1 h and then incubated with the primary antibody at 4 °C overnight. After washing with phosphate-buffered saline with 0.1% Tween 20 (PBST), the membrane was incubated with IRDye infrared secondary antibody (Li-Cor) for 1 h at room temperature. The membrane was washed with PBST again and detected with the Li-Cor Odyssey Infrared Imaging System.

2.8. Animal experiments

Animal experiments were carried out in accordance with *Guidelines for the Care and Use of Laboratory Animals* (NIH publication number 85-23) and the institutional guidelines of M.D. Anderson Cancer Center. Subcutaneous tumors were established in 6- to 8-week-old female nude mice (Charles River Laboratories Inc., Wilmington, MD) by inoculation of 1.5×10^6 H157 cells into the dorsal flank of each mouse. After the tumors grew to 3–5 mm in diameter, the mice were treated with intraperitoneal administration of NSC-743380 at a dose of 100 mg/kg/day (dissolved in 0.5 mL solvent containing 2.5% DMSO, 5% Tween 80, 5% ethanol and 10% polyethylene glycol 400) or solvent alone. Tumor volumes were calculated by using the formula $a \times b^2 \times 0.5$, where a and b represented the larger and smaller diameters, respectively. Mice were killed when the tumors grew to 15 mm in diameter. For testing whether STAT3 phosphorylation is suppressed, mice were treated with NSC-743380 for three days and tumors were harvested 24 h after the last treatment.

2.9. Immunohistochemical staining

Frozen sections of animal tumor specimens were used for immunostaining with antibodies against p-STAT3 (Invitrogen) according to the manufacturer's instruction. After incubation with primary antibody and wash with PBS, slides were incubated in 1:500 Alexa Fluor 488 goat anti-rabbit IgG antibody for 60 min at room temperature in a humid atmosphere in the dark. Slides were washed three times in PBS, then coverslip mounted with ProLong® Gold antifade reagent with DAPI (Invitrogen), and the coverslip edges sealed with non-fluorescent nail polish.

2.10. Statistical analysis

Each experiment or assay was performed at least two times, and representative examples are shown. Data were reported as means ± SEM. Statistical significance between treated

samples was calculated by using the Student's *t* test. Differences were considered statistically significant at $P < 0.05$.

3. Results

3.1. In vitro antitumor activity of NSC-743380 in lung cancer cell lines

The promising in vivo antitumor activity of NSC-743380 in renal tumor models led us to further investigate the antitumor activity of this compound in 50 NSCLC cell lines as well as its possible cytotoxicity in HBEC3KT (Fig. 1A). Cells were treated with 0.01–30 μM NSC-743380 for 72 h. Cell viability was determined by using the SRB assay. The results showed that NSC-743380 possessed selective cytotoxicity against a number of NSCLC cell lines (Fig. 1A). Among the 50 NSCLC cell lines tested, the median 50% inhibitory concentration (IC_{50}) for NSC-743380 was 2.63 μM, and the growth of several of these cell lines was remarkably inhibited by this agent. About 32% (16 of 50) of the cell lines had a IC_{50} of <1 μM. For the most sensitive cell lines, the IC_{50} was ≤10 nM, the lowest concentration tested in the study (Fig. 1A). The dose effects of NSC-743380 on cell viability in two sensitive lung cancer cell lines with KRAS mutation (H460 and H157), two resistant lung cancer cell lines (H322 and H1299), and a normal bronchial epithelial cell line (HBEC3KT) are shown in Fig. 1B. NSC-743380 markedly suppressed cell growth in a dose-dependent manner in H460 and H157 cells, with an IC_{50} of 0.32 μM and 0.2 μM, respectively, whereas in H322, H1299, and HBEC3KT cells, the IC_{50} was ≥10 μM.

To further characterize the inhibitory effects of NSC-743380 on cell proliferation, we performed cell cycle analyses with use of flow cytometry. In H460 and H157 cells, treatment with NSC-743380 for 24 h resulted in a dramatic increase of apoptotic cells in a dose-dependent manner (Fig. 1C). The percentage of apoptotic cell of H460 was about 30% at 0.3 μM NSC-743380 and about 50% at 1 μM NSC-743380, compared with 1% in the control cells treated with DMSO. The percentage of apoptotic cell of H157 was similar to that of H460 cells. NSC-743380 did not induce apoptosis in either resistant or normal cell lines. These results suggested that NSC-743380 can selectively suppress cell growth and induce apoptosis in some cancer cell lines, for example, in H460 and H157 cell lines.

3.2. NSC-743380 down-regulates constitutive STAT3 phosphorylation in the sensitive cell lines

Our recent study showed that NSC-743380 inhibited STAT3 phosphorylation in sensitive renal and breast cancer cells [19]. To investigate whether NSC-743380 also suppressed STAT3 phosphorylation in sensitive lung cancer cells, we treated the sensitive and resistant lung cancer cells with 1 μM NSC-743380 for 12 h; then the whole cell extracts were prepared, and phosphorylation of STAT3 at Y705 was examined by Western blot analysis. The results showed that NSC-743380 could completely suppress p-STAT3-Y705 expression in the sensitive cells, H460 and H157, whereas the effect on the basal STAT3 in these two cell lines was minimal (Fig. 2A).

In contrast, NSC-743380 had no detectable effect on expression of p-STAT3 in resistant cell lines H322 and H1299. Besides investigating the effects of NSC-743380 on the expression of p-STAT3-Y705, we tested its effects on the expression of JAK2 and Src, which are upstream regulators of STAT3 (Fig. 2A). NSC-743380 had minimal effect on levels of p-JAK2-(Y1007/Y1008), JAK2, p-Src-Y527, and Src in both the sensitive and resistant cell lines but had a moderate effect on the expression levels of p-Src-Y416 in the sensitive cell lines.

It is well known that poly(ADP-ribose) polymerase (PARP) plays a crucial role in cell death [20], and cleavage of PARP is an early event in apoptosis in intact cells [21]. Therefore, the

effect of NSC-743380 on the cleavage of PARP was also studied. An 89-kDa apoptotic fragment of PARP appeared after treatment in sensitive cell lines, whereas no such band was observed in the control groups. In resistant cell lines, NSC-743380 showed no effect on PARP cleavage (Fig. 2A, bottom).

Next, we evaluated the time- and dose-dependent changes of these proteins after NSC-743380 treatment in H460 and H157 cells (Fig. 2B and C). H460 and H157 cells were treated with 1 μM NSC-743380 for various time durations. Western blot analysis showed that the phosphorylation of STAT3 was down-regulated as early as 30 min after treatment and that constitutively active STAT3 (p-STAT3-Y705) was almost completely and durably inhibited after 2 h; STAT3 levels, however, showed almost no change with treatment. On the other hand, the expression of p-Src-Y416 was transiently inhibited at 30 min in both cell lines, followed by restoration to the control level at 2 h. There was moderate inhibition of p-Src-Y416 at 12 h in H460 cells. For both cell lines, there was mild expression of the cleaved PARP at 6 h. Cleaved PARP was strongly induced at 12 h.

Analysis of dose response showed that inhibition of p-STAT3-Y705 was dose-dependent and began at a dose of 0.1 μM while the inhibition of p-Src-Y416 was dose-dependent and began at a dose of 0.3 μM. Moreover, the induction of cleaved PARP also showed dose-dependent (Fig. 2C). Together, these results suggested that treatment with NSC-743380 induces inhibition of p-STAT3-Y705 before apoptosis is induced.

3.3. NSC-743380 induces ROS production in the sensitive cell lines

Our recent study showed that NSC-741909, an analogue of NSC-743380, induced ROS production in sensitive cancer cell lines and that ROS induction is associated with NSC-741909's antitumor activity [15,16]. It would therefore be of interest to investigate whether ROS would also be produced in sensitive cell lines by NSC-743380 treatment. Thus, H460 and H157 cells were treated either with various concentrations of NSC-743380 for 6 h (Fig. 3A) or with 1 μM NSC-743380 for different time durations, *i.e.*, 0.5, 2, and 6 h (Fig. 3B). ROS production was determined by a specific fluorescent dye, H_2DCF-DA. The results showed that NSC-743380 induced a large amount of ROS in both a dose- and time-dependent manner in both sensitive cell lines. In contrast, there was no ROS generation in the resistant H1299 cells or in normal HBEC3KT cells. Small amount of ROS began to generate as early as 2 h after treatment. ROS generation was about 3 times of the baseline level after 6 h. In addition, increasing the concentration of NSC-743380 increased ROS production substantially. Thus, as seen with NSC-741909, NSC-743380 triggers the generation of ROS in both a dose- and time-dependent manner in the sensitive cell lines.

3.4. Antioxidant blocks NSC-743380-induced ROS production and suppresses cell death

To investigate the possible roles of ROS production in NSC-743380-induced antitumor activity, we conducted tests to determine whether antioxidants could block ROS production and/or suppress the corresponding cell apoptosis. For this purpose, cells were pretreated with 10 μM NDGA [22], an antioxidant, for 1 h before treatment with 1 μM NSC-743380. The amount of ROS generated was measured 6 h after treatment with NSC-743380. As shown in Fig. 4A, NSC-743380-induced ROS production in H460 and H157 cells was substantially reduced by pretreatment with NDGA. Also, cell viability analyses of H460 (Fig. 4B) and H157 (Fig. 4C) revealed that NDGA blocked NSC-743380-induced growth suppression.

We also examined whether NDGA blocks NSC-743380-mediated apoptosis. To this end, H460 cells were treated with 1 μM NSC-743380 for 24 h, with or without prior addition of NDGA, and the percentage of apoptotic cells was analyzed by flow cytometry. Results

showed that pre-treatment of cells with NDGA markedly decreased the percentage of apoptotic cells compared with the cells treated with NSC-743380 alone (1% *vs.* 45%); in contrast, the use of NDGA alone showed no effect on apoptosis compared with not treating with NSC-743380 (1% *vs.* 1%) (Fig. 4D). Biochemical analysis using Western blot analysis confirmed the above observation since the addition of NDGA dramatically blocked the NSC-743380-induced cleavage of PARP (Fig. 4E). Nevertheless, NSC-743380-induced ROS and subsequent apoptosis were not blocked by pretreatment with antioxidants N-acetylcysteine or vitamin C (data not shown). Taken together, these results suggested that NSC-743380 may induce oxidative stress through a specific pathway that is affected by NDGA and that the increased ROS production is critical in NSC-743380-induced antitumor activity.

3.5. Down-regulation of STAT3 suppresses cell viability through ROS production

Because NSC-743380 can induce both ROS production and STAT3 inhibition, an intriguing question arises as to whether ROS generation is associated with STAT3 inhibition. To address this question, we first examined whether blocking ROS generation with antioxidants would affect STAT3 inhibition. To this end, H460 and H157 cells were treated with 10 μM NDGA for 1 h before treatment with 1 μM NSC-743380 for 12 h, and the p-STAT3-Y705 expression level was examined by Western blot analysis. We found that NDGA had no effect on the down-regulation of STAT3 phosphorylation induced by NSC-743380 in either cell line (Fig. 5), although at this combination, NDGA effectively blocked ROS generation (Fig. 4A). This result indicates that NSC-743380-induced STAT3 inhibition is independent of ROS generation.

We then examined the effect of knockdown of STAT3 on the production of ROS. As shown in Fig. 6A, STAT3-specific shRNA suppressed both p-STAT3-Y705 and STAT3 expression in H460 cells, whereas no such suppression of STAT3 was observed in cells transfected with control shRNA, thus indicating that shSTAT3 can knock down STAT3 effectively. Moreover, two fold increase in ROS production was induced by shSTAT3 compared with the control shRNA (Fig. 6B); in addition, the presence of shSTAT3 suppressed the cell viability, *i.e.*, *ca.* 70% reduction, in comparison with the control shRNA (Fig. 6C). Thus, knockdown of STAT3 is sufficient to induce ROS production and cytotoxicity in H460 cells.

Next, the effect of an antioxidant, NDGA, on ROS production and cell viability associated with STAT3 knocked down (shSTAT3) was studied. H460 cells were treated with NDGA followed by treatment with shSTAT3 for 48 h. ROS production was monitored by flow cytometry, and cell viability was determined by SRB assay. The results showed that NDGA can effectively block ROS production and cell growth suppression induced by shSTAT3 (Fig. 6B and C). The fact that the antioxidant's effect on cell viability coincides with the effect on ROS production suggests that in H460 cells, shSTAT3 can induce cell death through ROS production, which can be blocked by NDGA. This result suggested that STAT3 inhibition could be the upstream of ROS production and one of major antitumor mechanisms induced by NSC-743380.

3.6. In vivo antitumor activity of NSC-743380 in a lung cancer tumor model

To investigate the *in vivo* antitumor activity of NSC-743380 for lung cancer, we established subcutaneous tumors 6- to 8-week-old female nude mice by the inoculation of 1.5×10^6 H157 cells into the dorsal flank of each mouse. After the tumors grew to 3–5 mm in diameter, the mice were treated with intraperitoneal injections of solvent alone or 100 mg/kg/day of NSC-743380 for 10 days. The tumor volumes were calculated using the formula $a \times b^2 \times 0.5$, where a and b represent the larger and smaller diameters, respectively. The

results showed that NSC-743380 significantly suppressed tumor growth. In comparison with solvent, NSC-74330 suppressed growth of tumor volume by 80% (Fig. 7A). We also analyzed whether treatment with NSC-743380 suppressed STAT3 activity *in vivo*. For this purpose, 3 animals/group were sacrificed after treatment for three days and tumor tissues harvested for immunohistochemical staining of phosphor-STAT3. The result showed that treatment with NSC-743380 dramatically suppressed STAT3 phosphorylation in tumor tissues (Fig. 7B). Thus, NSC-743380 could effectively suppress STAT3 activity and tumor growth *in vivo* in lung cancers.

4. Discussion

Our results showed that NSC-743380 is highly active against 16 of the 50 lung cancer cell lines tested. The mechanisms underlying NSC-743380's selectivity is not yet clear. Although NCS-743380 was developed through analogue search of oncrasin-1 [12,13], a compound identified by synthetic lethality screening on KRAS mutant tumors, the antitumor activity of NSC-743380 in NCI-60 cell panel and in 50 NSCLC cell lines did not show a significant correlation with KRAS mutations. A subtype of cancer cells (about 25–30%), either with or without KRAS mutations, were highly sensitive to NSC-743380, in both NCI-60 panel and in the lung cancer cell lines tested here. It is noteworthy, however, that RAS activation signature was observed in a substantial number of primary lung adenocarcinomas with wild-type KRAS [23], suggesting functional activation of RAS signaling can be caused without RAS mutations. Whether NSC-743380's antitumor activity is associated with RAS activation signature remains to be determined. Mechanistic study on H460 and H157 cells demonstrated that NSC-743380 inhibited cell proliferation and induced apoptosis in sensitive lung cancer cells, accompanied by remarkable inhibition of the constitutively active STAT3 with time- and dose-dependent patterns. These data, together with previously published results [4,24–27], strongly confirm a model in which targeting constitutive STAT3 signaling effectively inhibits both cancer cell survival and the cancer-associated process [4,24–27]. Nevertheless, it is not clear if cellular levels of constitutively active STAT3 is associated with the susceptibility to NSC-743380, although our study on the four lung cancer lines tested here and four breast and renal cancer cell lines tested in a recent study [19] all showed that sensitive cells have relatively high levels of p-STAT3-Y-705. A survey on levels of constitutively active STAT3 in NCI-60 cell lines and in the 50 lung cancer cell lines tested may provide an answer. Alternatively, correlation analysis on gene expression levels and susceptibility to NSC-743380 may provide clues for the selectivity. However, NSC-743380 has either minor or transient effects on the upstream regulators of the STAT3 signaling pathway, the tyrosine kinases JAK2 and Src, suggesting that the persistent inhibition of p-STAT3-Y705 by NSC-743380 might be JAK2- and Src-independent. Unlike dasatinib, a Src family kinase inhibitor that induced sustained inhibition of p-Src-Y416 but transient inhibition of p-STAT3-Y705 [28], NSC-743380 induced sustained inhibition of STAT3 but transient inhibition of p-Src-Y416, suggesting that Src family kinases are not the primary targets of NSC-743380. Whether reactivation of Src is caused by a feedback of STAT3 inhibition is not yet clear. It is also not clear whether NSC-743380 acts through interfering functions of SH2 domain of STAT3, as was reported for some other STAT3 inhibitors [29,30]. Thus, the exact mechanism of NSC-743380 inhibition of STAT3 remains to be determined. Since multiple types of cancers, including multiple myeloma [31], head and neck cancers [3], lymphomas, and leukemia [32], also have constitutively active STAT3, the suppression of constitutively active STAT3 in lung cancer cells raises the possibility that NSC-743380 may also inhibit constitutively activated STAT3 in other types of cancer cells.

ROS are produced as byproducts of normal oxygen metabolism. Normal cells produce low concentrations of ROS, which can be effectively neutralized by the potent antioxidant

system of the cells. In contrast, cancer cells produce elevated levels of ROS because of their increased metabolic activity, resulting in a state of chronic oxidative stress [33]. This abnormal increase in ROS renders cancer cells very sensitive to oxidative stress inducers [34]. Excessive levels of ROS beyond the antioxidant capacity of cancer cells can readily induce cell cycle arrest and apoptosis [6,9]. ROS induced DNA damage and subsequent overactivation of PARP may lead to excessive consumption of ATP and NAD^+ and translocation of apoptosis-inducing factor from mitochondria to nucleus, and finally apoptosis [35]. In fact, PARP inhibitors were reported to completely protect lymphocytes from radical-induced apoptosis [4], suggesting that PARP is one of downstream mediators of ROS-induced apoptosis. Acute generation of ROS is frequently observed in apoptosis induced by various anticancer agents [36–40]. These agents further elevate ROS levels beyond a threshold, ultimately triggering apoptosis in the cancer cells. However, normal cells are less sensitive to agents that induce oxidative stress due to their low basal ROS output and high antioxidant capacity. This biochemical difference between normal and cancer cells may constitute a basis for modulating cellular ROS as an anticancer therapeutic strategy to selectively kill cancer cells.

The present study demonstrated that NSC-743380 can induce ROS overproduction in the H460 and H157 sensitive lung cancer cell lines in a dose- and time-dependent manner but cannot induce ROS in the normal cell line, HBEC3KT, or in the resistant cell line, H1299. Furthermore, NSC-743380-induced ROS production can be blocked by NDGA, a ROS scavenger, in both sensitive cell lines. Parallel to this, apoptosis induced by NSC-743380 in the sensitive cell lines is ROS-dependent since NDGA can also block the NSC-743380-mediated apoptotic effect in H460 cells. These results are consistent to our previous finding on antagonist effect of NDGA to an analogue NSC-741909 [15,16], indicating that ROS generation is critical in NSC-743380-induced antitumor activity in lung cancer cells.

Because NSC-743380 induced both STAT3 inhibition and ROS generation, it would be interesting to investigate whether these two effects are associated. The effect of ROS on STAT3 phosphorylation and activation is controversial. ROS has been reported to activate the JAK/Stat pathway through inactivation of tyrosine phosphatases [41–43]. However, oxidation of cysteine residues in JAK and STAT3 proteins themselves was reported to inhibit phosphorylation and activation of these proteins [44–46]. Our results showed that scavenging ROS with some antioxidants block NSC-743380-induced cell killing but had no notable effect on NSC-743380-induced STAT3 inhibition, suggesting that STAT3 inhibition is independent of NSC-743380-mediated ROS generation. We also investigated whether STAT3 inhibition was sufficient to induce ROS generation. Our results showed that knockdown of STAT3 by STAT3-specific shRNA was sufficient to induce ROS production and suppress cell growth, which was also blocked by NDGA. This result suggested that STAT3 inhibition might be upstream of ROS induction.

Indeed, STAT3 was reported to scavenge ROS by upregulating manganese superoxide dismutase and its enzyme activity [47] and to suppress Fas-induced oxidative stress [48]. Furthermore, mitochondrial STAT3, which supports RAS-mediated transformation, may involve in regulating glucose and redox metabolisms [49]. Suppression of STAT3 has been found to induce oxidative stress in astrocytes and in myeloid-derived suppressor cells [50,51]. These results, along with our own, suggested that ROS could be a downstream mediator of STAT3 signaling and that suppression of STAT3 might be an effective approach to modulate cellular oxidative stress for therapeutic benefit.

Acknowledgments

We thank Tamara Locke for her editorial review of this manuscript.

Abbreviations

H_2DCFDA	2′,7′-dichlorofluorescein diacetate
JNK	c-Jun N-terminal kinase
HBEC3KT	normal human bronchial epithelial
NDGA	nordihydroguaiaretic acid
PI	propidium iodide
PARP	poly(ADP-ribose) polymerase
ROS	reactive oxygen species
STAT3	signal transducer and activator of transcription 3
SRB	sulforhodamine B

References

1. Zhong Z, Wen Z, Darnell JE Jr. Stat3: a STAT family member activated by tyrosine phosphorylation in response to epidermal growth factor and interleukin-6. Science. 1994; 264:95–98. [PubMed: 8140422]
2. Yu H, Jove R. The STATs of cancer – new molecular targets come of age. Nat Rev Cancer. 2004; 4:97–105. [PubMed: 14964307]
3. Song JI, Grandis JR. STAT signaling in head and neck cancer. Oncogene. 2000; 19:2489–2495. [PubMed: 10851047]
4. Thoren FB, Romero AI, Hellstrand K. Oxygen radicals induce poly(ADP-ribose) polymerase-dependent cell death in cytotoxic lymphocytes. J Immunol. 2006; 176:7301–7307. [PubMed: 16751373]
5. Amann J, Kalyankrishna S, Massion PP, Ohm JE, Girard L, Shigematsu H, et al. Aberrant epidermal growth factor receptor signaling and enhanced sensitivity to EGFR inhibitors in lung cancer. Cancer Res. 2005; 65:226–235. [PubMed: 15665299]
6. Schumacker PT. Reactive oxygen species in cancer cells: live by the sword, die by the sword. Cancer Cell. 2006; 10:175–176. [PubMed: 16959608]
7. Ushio-Fukai M, Nakamura Y. Reactive oxygen species and angiogenesis: NADPH oxidase as target for cancer therapy. Cancer Lett. 2008; 266:37–52. [PubMed: 18406051]
8. Clerkin JS, Naughton R, Quiney C, Cotter TG. Mechanisms of ROS modulated cell survival during carcinogenesis. Cancer Lett. 2008; 266:30–36. [PubMed: 18372105]
9. Trachootham D, Lu W, Ogasawara MA, Nilsa RD, Huang P. Redox regulation of cell survival. Antioxid Redox Signal. 2008; 10:1343–1374. [PubMed: 18522489]
10. Ozben T. Oxidative stress and apoptosis: impact on cancer therapy. J Pharm Sci. 2007; 96:2181–2196. [PubMed: 17593552]
11. Renschler MF. The emerging role of reactive oxygen species in cancer therapy. Eur J Cancer. 2004; 40:1934–1940. [PubMed: 15315800]
12. Guo W, Wu S, Liu J, Fang B. Identification of a small molecule with synthetic lethality for K-ras and protein kinase C iota. Cancer Res. 2008; 68:7403–7408. [PubMed: 18794128]
13. Guo W, Wu S, Wang L, Wang RY, Wei X, Liu J, et al. Interruption of RNA processing machinery by a small compound, 1-[(4-chlorophenyl)methyl]-1H-indole-3-carboxaldehyde (oncrasin-1). Mol Cancer Ther. 2009; 8:441–448. [PubMed: 19208825]
14. Wu S, Wang L, Guo W, Liu X, Liu J, Wei X, et al. Analogues and derivatives of oncrasin-1, a novel inhibitor of the C-terminal domain of RNA polymerase II and their antitumor activities. J Med Chem. 2011; 54:2668–2679. [PubMed: 21443218]
15. Wei X, Guo W, Wu S, Wang L, Huang P, Liu J, et al. Oxidative stress in NSC-741909-induced apoptosis of cancer cells. J Transl Med. 2010; 8:37. [PubMed: 20398386]

16. Guo W, Wei X, Wu S, Wang L, Peng H, Wang J, et al. Antagonistic effect of flavonoids on NSC-741909-mediated antitumor activity via scavenging of reactive oxygen species. Eur J Pharmacol. 2010; 649:51–58. [PubMed: 20854805]

17. Ramirez RD, Sheridan S, Girard L, Sato M, Kim Y, Pollack J, et al. Immortalization of human bronchial epithelial cells in the absence of viral oncoproteins. Cancer Res. 2004; 64:9027–9034. [PubMed: 15604268]

18. Pauwels B, Korst AE, de Pooter CM, Pattyn GG, Lambrechts HA, Baay MF, et al. Comparison of the sulforhodamine B assay and the clonogenic assay for in vitro chemoradiation studies. Cancer Chemother Pharmacol. 2003; 51:221–226. [PubMed: 12655440]

19. Guo W, Wu S, Wang L, Wei X, Liu X, Wang J, et al. Antitumor activity of a novel oncrasin analogue is mediated by JNK activation and STAT3 inhibition. PLoS One. 2011; 6:e28487. [PubMed: 22174819]

20. Lazebnik YA, Kaufmann SH, Desnoyers S, Poirier GG, Earnshaw WC. Cleavage of poly(ADP-ribose) polymerase by a proteinase with properties like ICE. Nature. 1994; 371:346–347. [PubMed: 8090205]

21. Kaufmann SH, Desnoyers S, Ottaviano Y, Davidson NE, Poirier GG. Specific proteolytic cleavage of poly(ADP-ribose) polymerase: an early marker of chemotherapy-induced apoptosis. Cancer Res. 1993; 53:3976–3985. [PubMed: 8358726]

22. Guzman-Beltran S, Espada S, Orozco-Ibarra M, Pedraza-Chaverri J, Cuadrado A. Nordihydroguaiaretic acid activates the antioxidant pathway Nrf2/HO-1 and protects cerebellar granule neurons against oxidative stress. Neurosci Lett. 2008; 447:167–171. [PubMed: 18852027]

23. Barbie DA, Tamayo P, Boehm JS, Kim SY, Moody SE, Dunn IF, et al. Systematic RNA interference reveals that oncogenic KRAS-driven cancers require TBK1. Nature. 2009; 462:108–112. [PubMed: 19847166]

24. Grossklaus DJ, Shappell SB, Gautam S, Smith JA Jr, Cookson MS. Ratio of free-to-total prostate specific antigen correlates with tumor volume in patients with increased prostate specific antigen. J Urol. 2001; 165:455–458. [PubMed: 11176395]

25. Rajendran P, Ong TH, Chen L, Li F, Shanmugam MK, Vali S, et al. Suppression of signal transducer and activator of transcription 3 activation by butein inhibits growth of human hepatocellular carcinoma in vivo. Clin Cancer Res. 2011; 17:1425–1439. [PubMed: 21131551]

26. Free Radic Biol Med; Abstracts of the Society for Free Radical Biology and Medicine (SFRBM) 12th Annual Meeting; November 16–20, 2005; Austin, Texas, USA. 2005. p. S1-S177.

27. Davies KJ, Pryor WA. The evolution of free radical biology & medicine: a 20-year history. Free Radic Biol Med. 2005; 39:1263–1264. [PubMed: 16257637]

28. Sen B, Saigal B, Parikh N, Gallick G, Johnson FM. Sustained Src inhibition results in signal transducer and activator of transcription 3 (STAT3) activation and cancer cell survival via altered Janus-activated kinase-STAT3 binding. Cancer Res. 2009; 69:1958–1965. [PubMed: 19223541]

29. Siddiquee K, Zhang S, Guida WC, Blaskovich MA, Greedy B, Lawrence HR, et al. Selective chemical probe inhibitor of Stat3, identified through structure-based virtual screening, induces antitumor activity. Proc Natl Acad Sci USA. 2007; 104:7391–7396. [PubMed: 17463090]

30. Zhao W, Jaganathan S, Turkson J. A cell-permeable Stat3 SH2 domain mimetic inhibits Stat3 activation and induces antitumor cell effects in vitro. J Biol Chem. 2010; 285:35855–35865. [PubMed: 20807764]

31. Bhardwaj A, Sethi G, Vadhan-Raj S, Bueso-Ramos C, Takada Y, Gaur U, et al. Resveratrol inhibits proliferation, induces apoptosis, and overcomes chemoresistance through down-regulation of STAT3 and nuclear factor-kappaB-regulated antiapoptotic and cell survival gene products in human multiple myeloma cells. Blood. 2007; 109:2293–2302. [PubMed: 17164350]

32. Zhang Q, Raghunath PN, Xue L, Majewski M, Carpentieri DF, Odum N, et al. Multilevel dysregulation of STAT3 activation in anaplastic lymphoma kinase-positive T/null-cell lymphoma. J Immunol. 2002; 168:466–474. [PubMed: 11751994]

33. Szatrowski TP, Nathan CF. Production of large amounts of hydrogen peroxide by human tumor cells. Cancer Res. 1991; 51:794–798. [PubMed: 1846317]

34. Trachootham D, Zhou Y, Zhang H, Demizu Y, Chen Z, Pelicano H, et al. Selective killing of oncogenically transformed cells through a ROS-mediated mechanism by beta-phenylethyl isothiocyanate. Cancer Cell. 2006; 10:241–252. [PubMed: 16959615]
35. van Wijk SJ, Hageman GJ. Poly(ADP-ribose) polymerase-1 mediated caspase-independent cell death after ischemia/reperfusion. Free Radic Biol Med. 2005; 39:81–90. [PubMed: 15925280]
36. Huang P, Feng L, Oldham EA, Keating MJ, Plunkett W. Superoxide dismutase as a target for the selective killing of cancer cells. Nature. 2000; 407:390–395. [PubMed: 11014196]
37. Pelicano H, Feng L, Zhou Y, Carew JS, Hileman EO, Plunkett W, et al. Inhibition of mitochondrial respiration: a novel strategy to enhance drug-induced apoptosis in human leukemia cells by a reactive oxygen species-mediated mechanism. J Biol Chem. 2003; 278:37832–37839. [PubMed: 12853461]
38. Tan S, Sagara Y, Liu Y, Maher P, Schubert D. The regulation of reactive oxygen species production during programmed cell death. J Cell Biol. 1998; 141:1423–1432. [PubMed: 9628898]
39. Carmody RJ, Cotter TG. Signalling apoptosis: a radical approach. Redox Rep. 2001; 6:77–90. [PubMed: 11450987]
40. Feinendegen LE. Reactive oxygen species in cell responses to toxic agents. Hum Exp Toxicol. 2002; 21:85–90. [PubMed: 12102502]
41. Simon AR, Rai U, Fanburg BL, Cochran BH. Activation of the JAK-STAT pathway by reactive oxygen species. Am J Physiol. 1998; 275:C1640–C1652. [PubMed: 9843726]
42. Liu T, Castro S, Brasier AR, Jamaluddin M, Garofalo RP, Casola A. Reactive oxygen species mediate virus-induced STAT activation: role of tyrosine phosphatases. J Biol Chem. 2004; 279:2461–2469. [PubMed: 14578356]
43. Carballo M, Conde M, El Bekay R, Martin-Nieto J, Camacho MJ, Monteseirin J, et al. Oxidative stress triggers STAT3 tyrosine phosphorylation and nuclear translocation in human lymphocytes. J Biol Chem. 1999; 274:17580–17586. [PubMed: 10364193]
44. Mamoon NM, Smith JK, Chatti K, Lee S, Kundrapu K, Duhe RJ. Multiple cysteine residues are implicated in Janus kinase 2-mediated catalysis. Biochemistry. 2007; 46:14810–14818. [PubMed: 18052197]
45. Dixit D, Sharma V, Ghosh S, Koul N, Mishra PK, Sen E. Manumycin inhibits STAT3, telomerase activity, and growth of glioma cells by elevating intracellular reactive oxygen species generation. Free Radic Biol Med. 2009; 47:364–374. [PubMed: 19409983]
46. Li L, Cheung SH, Evans EL, Shaw PE. Modulation of gene expression and tumor cell growth by redox modification of STAT3. Cancer Res. 2010; 70:8222–8232. [PubMed: 20807804]
47. Negoro S, Kunisada K, Fujio Y, Funamoto M, Darville MI, Eizirik DL, et al. Activation of signal transducer and activator of transcription 3 protects cardiomyocytes from hypoxia/reoxygenation-induced oxidative stress through the upregulation of manganese superoxide dismutase. Circulation. 2001; 104:979–981. [PubMed: 11524388]
48. Haga S, Terui K, Zhang HQ, Enosawa S, Ogawa W, Inoue H, et al. Stat3 protects against Fas-induced liver injury by redox-dependent and -independent mechanisms. J Clin Invest. 2003; 112:989–998. [PubMed: 14523036]
49. Gough DJ, Corlett A, Schlessinger K, Wegrzyn J, Larner AC, Levy DE. Mitochondrial STAT3 supports Ras-dependent oncogenic transformation. Science. 2009; 324:1713–1716. [PubMed: 19556508]
50. Sarafian TA, Montes C, Imura T, Qi J, Coppola G, Geschwind DH, et al. Disruption of astrocyte STAT3 signaling decreases mitochondrial function and increases oxidative stress in vitro. PLoS One. 2010; 5:e9532. [PubMed: 20224768]
51. Corzo CA, Cotter MJ, Cheng P, Cheng F, Kusmartsev S, Sotomayor E, et al. Mechanism regulating reactive oxygen species in tumor-induced myeloid-derived suppressor cells. J Immunol. 2009; 182:5693–5701. [PubMed: 19380816]

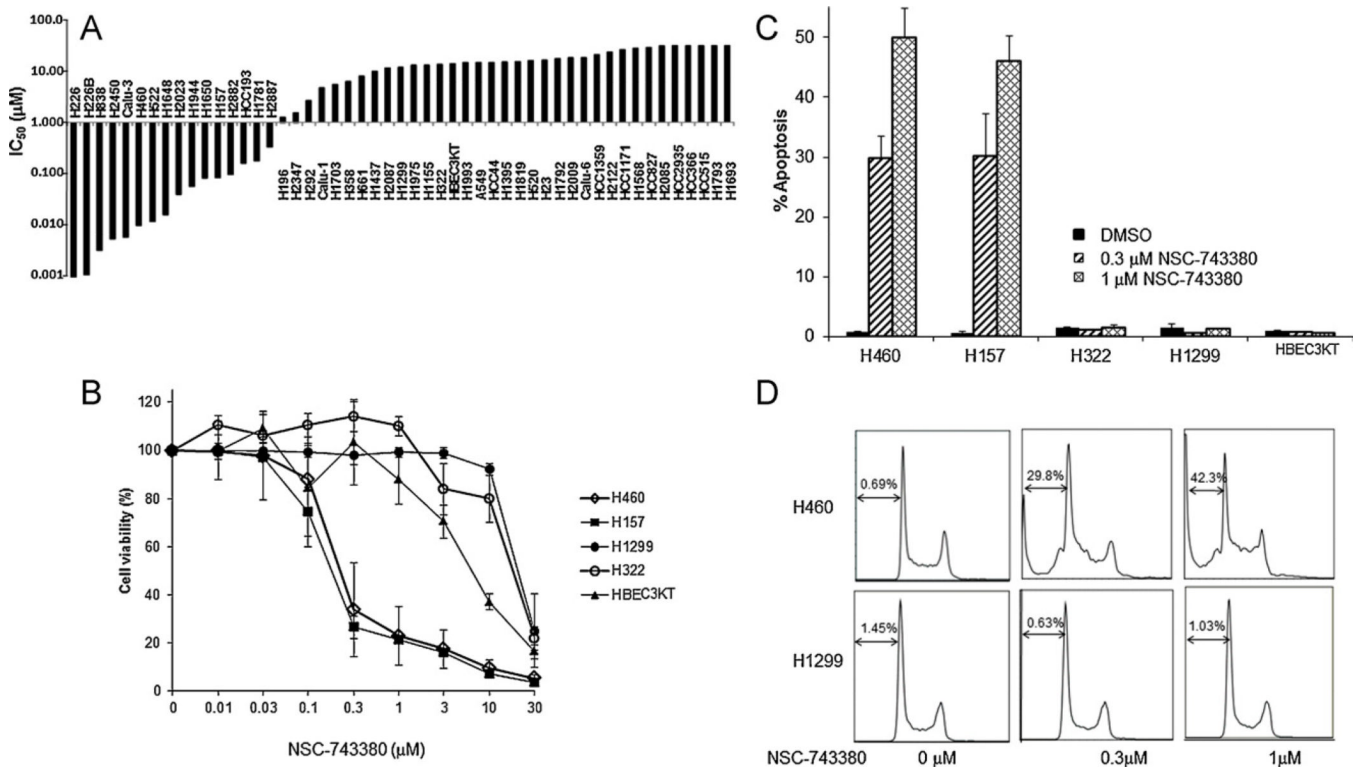

Fig. 1.

Cytotoxicity of NSC-743380. (A) Cytotoxicity of NSC-743380 for 50 lung cancer cell lines. Bar graph shows the calculated IC_{50} for 50 lung cancer lines. (B) Cell growth suppression induced by NSC-743380 in various cell lines. Two sensitive cell lines (H460 and H157), two resistant cell lines (H1299 and H322), and a normal cell line (HBEC3KT) were treated with various concentrations of NSC-743380 (0.01–30 μM). Cell viability was determined 72 h after treatment. Cells treated with dimethylsulfoxide alone were used as controls, and their viability was set to 100%. (C) Apoptosis induced by either 0.3 μM or 1 μM NSC-743380 in both sensitive cell lines (H460 and H157) and resistant cell lines (H1299 and H322). Cells were treated with various concentrations of NSC-743380 for 24 h and then harvested and incubated with propidium iodide for 30 min. Samples were then subjected to flow cytometry analysis. Percentage of apoptosis was shown as bar graph. Each data point represents the mean ± SD of three independent experiments. The representative histograms were shown in (D).

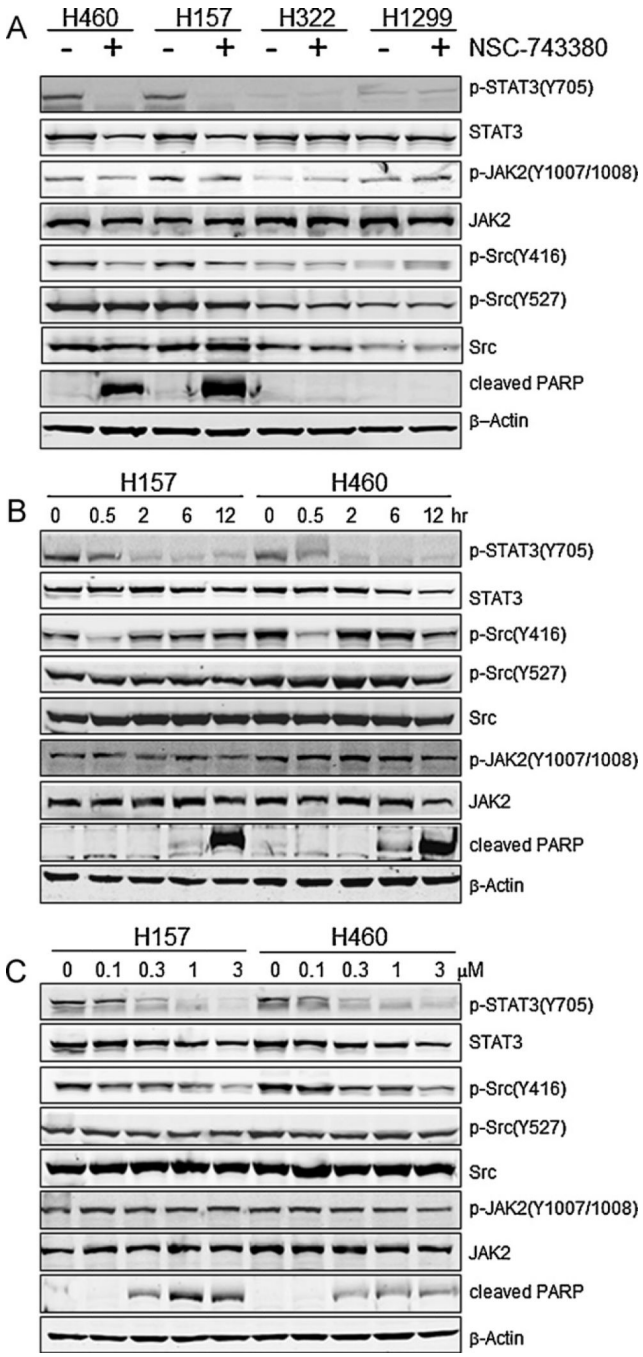

Fig. 2.

Down-regulation of p-STAT3-Y705 by NSC-743380. (A) Both sensitive and resistant cells were treated with 1 μM NSC-743380 for 12 h, and cell lysates were prepared. Expression levels of p-STAT3-Y705, STAT3, p-Src-Y416, p-Src-Y527, Src, p-JAK2-(Y1007/1008), JAK2, and cleaved PARP were determined by Western blot analysis. β-Actin was used as a loading control. (B) Time-dependent changes of proteins mentioned above. H460 and H157 were treated with 1 μM NSC-743380 at different time duration, 0.5, 2, 6, and 12 h, respectively. (C) Dose-dependent changes of proteins mentioned above. H460 and H157 cells were treated with various concentrations of NSC-743380, *i.e.*, 0.1, 0.3, 1, and 3 μM, respectively, for 12 h.

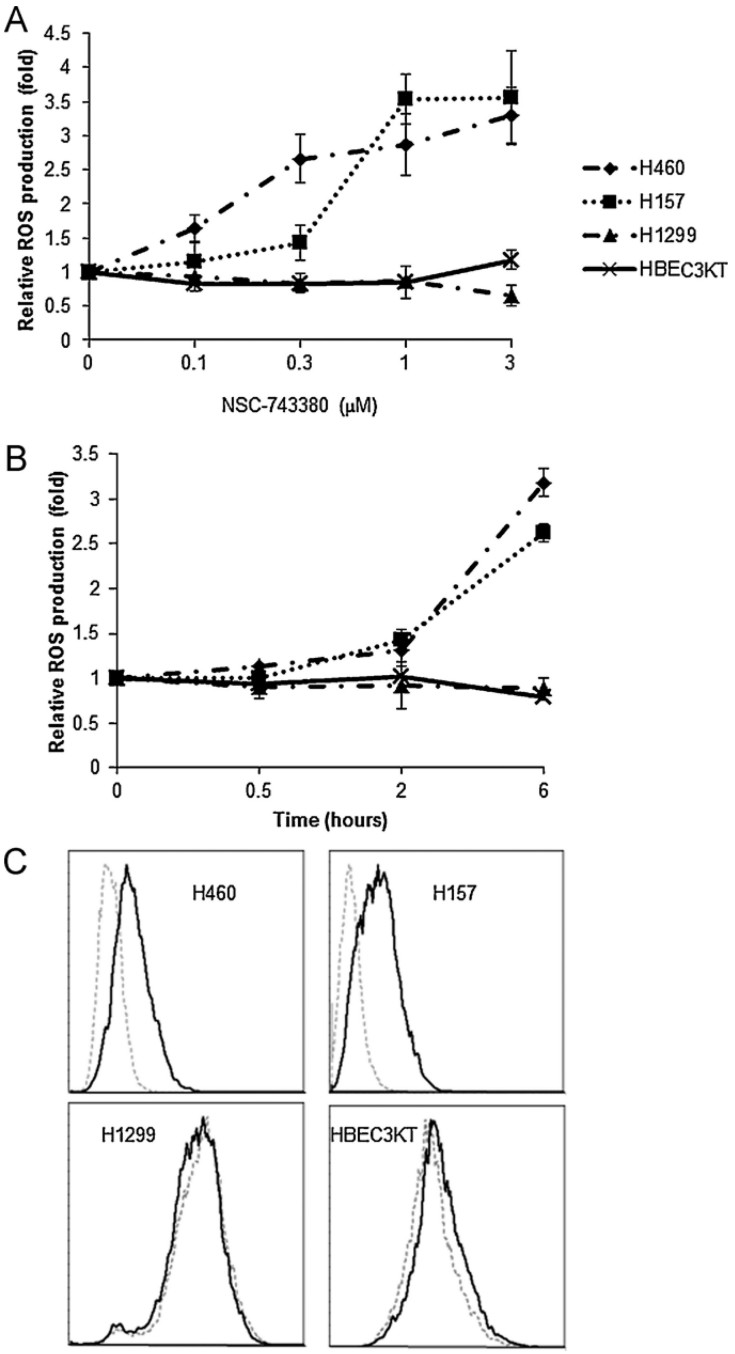

Fig. 3.

ROS generation in H460, H157, H1299, and HBEC3KT cells after treatment with NSC-743380. (A and B) Dose- and time-dependent ROS production induced by NSC-743380. Cells were treated with different concentrations of NSC-743380 for 6 h (A) or with 1 μM NSC-743380 at various periods (B). Cells were then stained by H_2DCF-DA and subjected to flow cytometry analysis. Cells treated with dimethylsulfoxide (DMSO) were used as controls, and their mean fluorescent intensity was set at 1. Each data point represents the mean ± SD of two independent experiments. (C) Representative histograms of ROS induction by NSC-743380 were shown, grey dot lines represent DMSO control and black lines represent ROS production after treatment with 3 μM NSC-743380 for 6 h.

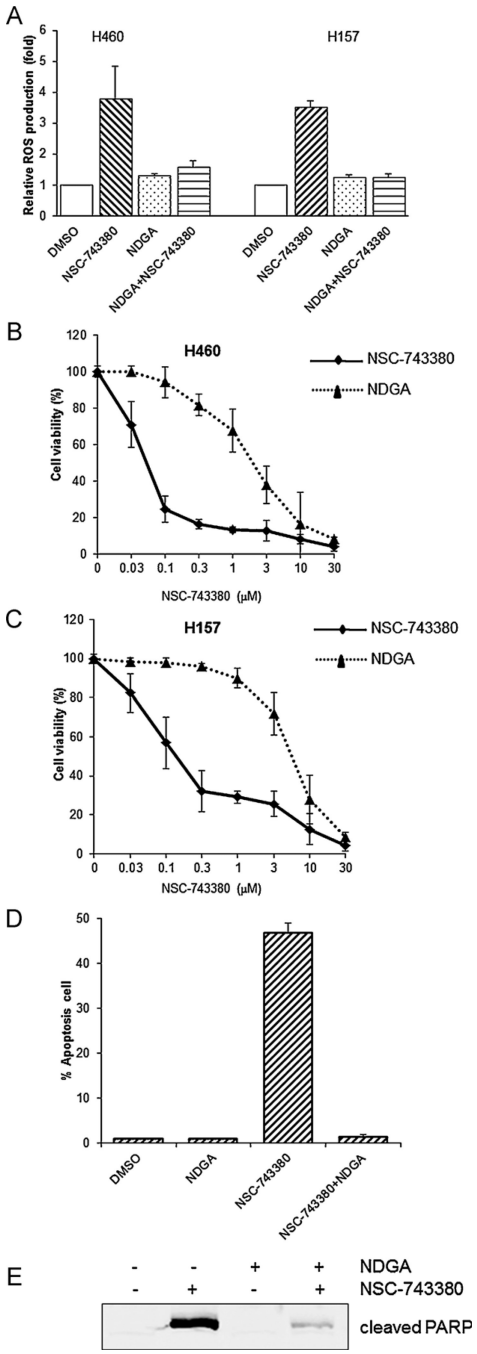

Fig. 4.

Antagonistic effects of NDGA on NSC-743380-induced ROS generation and apoptosis. Cells were pretreated with or without 10 μM NDGA for 1 h and then treated with 1 μM NSC-743380 for 6 h. Cells treated with DMSO were used as controls. (A) ROS generation was monitored by flow cytometry after treatment with NSC-743380. (B and C) Cell viability was determined by sulforhodamine B assay. (D) Cell killing effect was examined by flow cytometry, the percentage of apoptosis cell was shown as bar graph. (E) PARP cleavage was determined by Western blot analysis. The experimental settings and calculation methods were the same as those mentioned above.

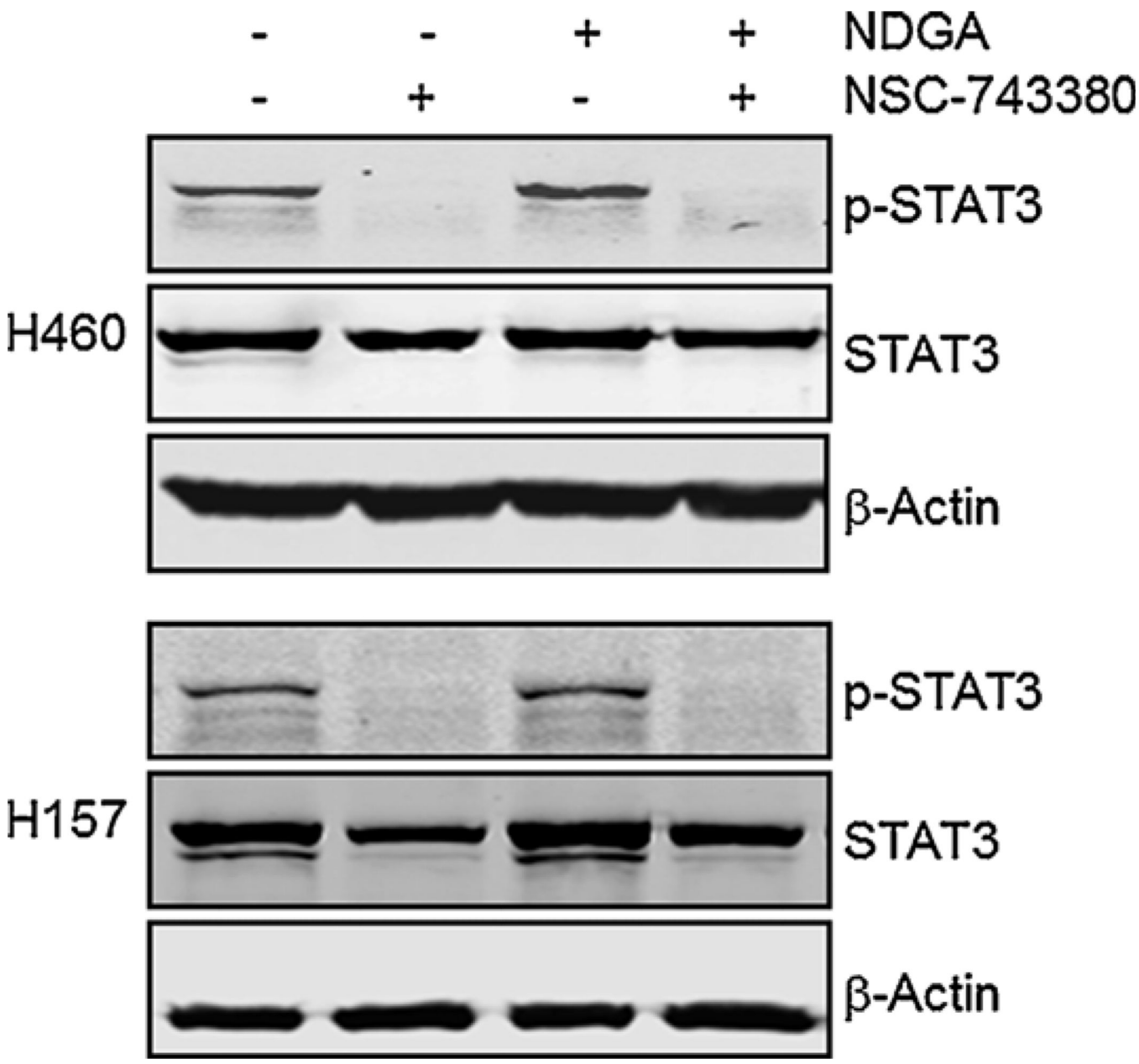

Fig. 5.

Effect of NDGA on NSC-743380-induced down-regulation of p-STAT3-Y705. H460 and H157 cells were pretreated with 10 μM NDGA for 1 h and then treated with 1 μM NSC-743380 for 12 h. Whole cell lysate from both cells were prepared for Western blot analysis of p-STAT3-Y705 and STAT3. β-Actin was used as a loading control.

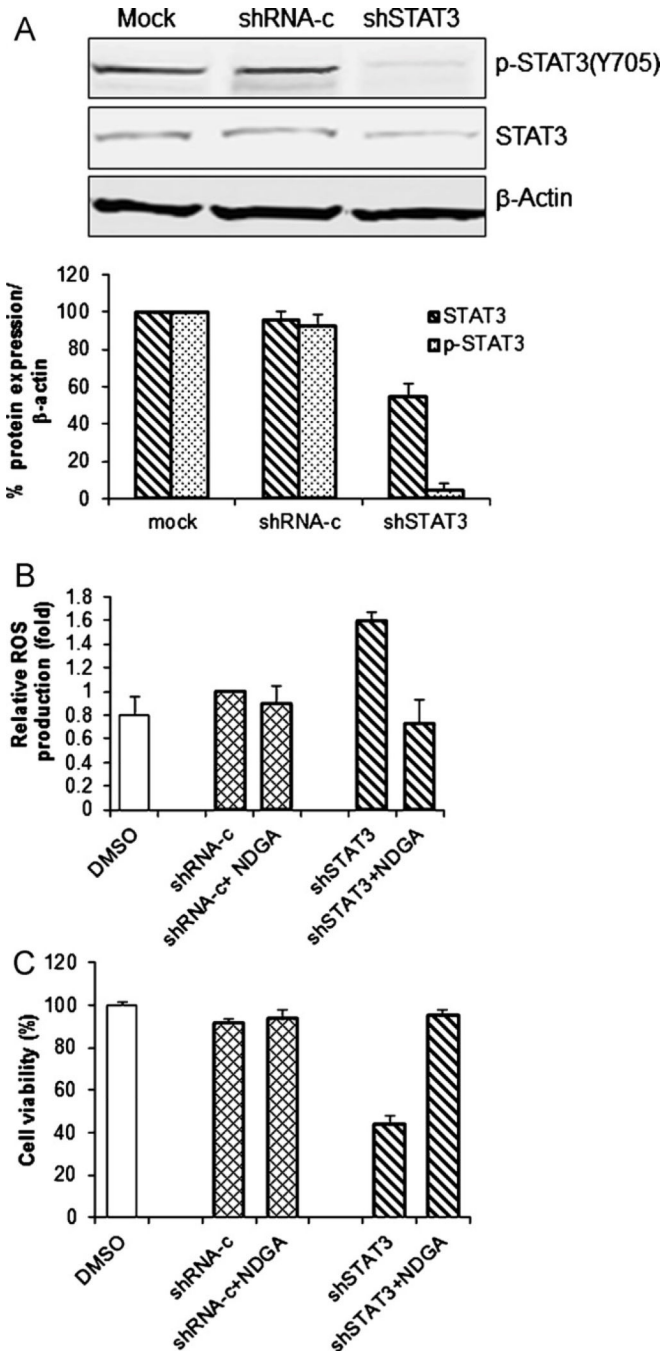

Fig. 6.

Down-regulation of STAT3 suppresses cell viability through ROS production. H460 cells were treated with shSTAT3 for 48 h. Cells treated with shRNA-control (shRNA-c) were used as a control. (A) Whole cell lysate was prepared and Western blot analysis was performed to determine protein levels using indicated antibodies. β-Actin was used as a loading control. The ratios of STAT3 to β-actin and p-STAT3 to β-actin are shown in bar graph. (B and C) H460 cells were pretreated with or without 10 μM NDGA for 1 h before treatment with shRNA for 48 h. (B) Cells were harvested and stained with H_2DCF-DA; ROS production was then determined by flow cytometry. Mean fluorescence intensity in cells transfected with shRNA-control was set as 1. (C) The percentage of viable cells was

determined by the SRB assay. Cells treated with shRNA-control were used as a control, with viability set at 100%. The values shown represent the mean ± SD of two determinations.

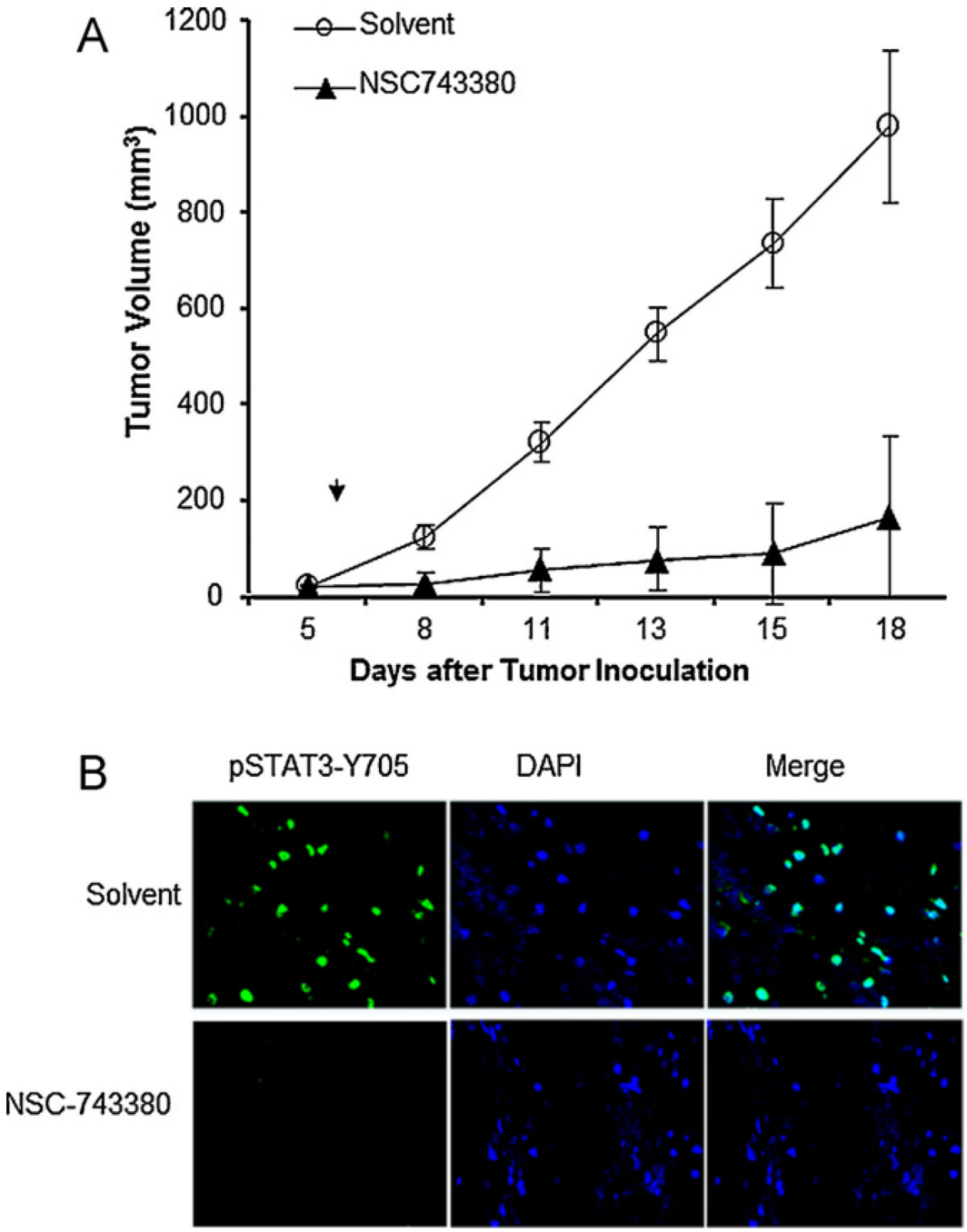

Fig. 7.

In vivo antitumor activity of NSC-743380. (A) Suppression of tumor growth. Mice bearing subcutaneous tumors derived from H157 cells were treated with NSC-743380 or solvent. Tumor volumes were monitored over time after the treatments. The values are the means ± SD of data from 8 mice per group. (B) Expression of p-STAT3 in tumors treated with NSC-743380 or solvent. The nucleus of tumor cell was revealed by DAPI staining.